

THE CONVEX BACK-SCATTERING SUPPORT

HOUSSEM HADDAR ^{*}, STEVEN KUSIAK [†], AND JOHN SYLVESTER [‡]

Abstract. A monochromatic, i.e. fixed frequency, back-scattering kernel measured at all angles does not uniquely determine the index of refraction in an inhomogeneous medium, nor can it guarantee any upper bound on the support of the inhomogeneity. We show that it is possible to associate with any such kernel its *convex back-scattering support*, a convex set which must be a subset of the convex hull of the support of any inhomogeneity with that back-scattering kernel. For the Born approximation, we further demonstrate that there is an inhomogeneity supported in any neighborhood of the convex back-scattering support which has exactly that back-scattering kernel. Lastly, we discuss a practical implementation of these results and include a numerical example.

Key words. inverse scattering, Helmholtz equation, partial differential equations, back-scattering

AMS subject classifications. 81U40, 74J25, 65N21, 35P25

1. Introduction. The goal of inverse scattering is to use acoustic or electromagnetic waves to deduce properties of a scatterer from remote observations. Exactly which properties and how well we can deduce them depend on exactly what scattering data we measure. In this paper the measured data is the back-scattered far field at all angles and a single frequency. A back-scattering experiment requires only a single sensor, which acts as both the source and receiver. The sensor radiates at a single temporal frequency, and measures the amplitude and phase of the resulting time harmonic field. We can move the sensor to an arbitrary location on a sphere of large radius that surrounds the scatterer and repeat the experiment. The complex field (amplitude and phase) measured at each point on the sphere is the back-scattering data.

We will use the Helmholtz equation as our model for the propagation of time harmonic waves,

$$(1.1) \quad (\Delta + k^2 n^2(x))u = 0, \quad x \in \mathbb{R}^d, \quad d \geq 2$$

Here, $n(x) = \frac{c_0}{c(x)}$ is the index of refraction, which is the ratio of the wave speed in the vacuum to that in the medium, while $k = 2\pi/\lambda$ denotes the wavenumber. It will be convenient to define the scattering potential, $q(x) := k^2(1 - n^2)$, and to rewrite (1.1) as

$$(1.2) \quad (\Delta + k^2)u = qu$$

$$(1.3) \quad u = e^{ik\Theta \cdot x} + u_{sc}$$

$$(1.4) \quad u_{sc} \sim \frac{e^{ikr}}{r^{\frac{d-1}{2}}} s_q(\Phi, \Theta), \quad |x| = r \rightarrow \infty$$

Equation (1.3) expresses the fact that, although the sensor, located at $\Theta \in S^{d-1}$, acts as a point source and emits a spherical wave, the sphere is far enough from

^{*}Laboratoire POems, UMR 2706 CNRS/ENSTA/INRIA, INRIA, Domaine de Voluceau-Rocquencourt, BP 105, 78153 Le Chesnay cedex, France (houssem.haddar@inria.fr)

[†]MIT Lincoln Laboratory, Lexington MA, 02420-9180, (kusiak@ll.mit.edu). This work completed while the author was a CNRS post-doctoral fellow at Laboratoire POems, UMR 2706 CNRS/ENSTA/INRIA, ENSTA, 32 Boulevard Victor, 75739 Paris cedex 15, France

[‡]Department of Mathematics, University of Washington, Seattle, WA 98195, Research supported by NSF Grant DMS-0099838 and ONR Grant N00014-93-1-0295 (sylvest@math.washington.edu)

the scatterer that the incident wave appears to be a plane wave in a neighborhood of the scatterer. Equation (1.4) expresses the asymptotics of the *outgoing* scattered wave¹. The field measured by an additional dislocated sensor positioned at $\Phi \in S^{d-1}$ is denoted by $s_q(\Phi, \Theta)$. This quantity is called the *scattering kernel*. We define the back-scattering kernel as $s(\Theta) := s_q(\Theta, -\Theta)$. The back-scattering kernel represents the complex time-harmonic scattered field measured at the source position. We will discuss both the back-scattering kernel and what we will call the *Born-back-scattering* kernel. We denote the latter quantity by $b(\Theta) := b_q(\Theta, -\Theta)$, and remark that it is the analog of $s(\Theta)$ in the Born, or single scattering, approximation. In both cases, a main feature is that the fixed frequency back-scattering data does not uniquely determine the scattering potential $q(x)$. Indeed, the Born-back-scattering kernel is equal to a constant (in Θ) multiple of the Fourier transform of q , restricted to the sphere of radius $2k$, i.e.

$$(1.5) \quad b(\Theta) = \frac{k^{d-2}}{2i} \widehat{q}(2k\Theta)$$

We learn from (1.5) that, as long as $g(x)$ is a smooth compactly supported function, then $\tilde{q} = (\Delta + (2k)^2)g$ has zero Born-back-scattering kernel, so that

$$(1.6) \quad b_{q+\tilde{q}}(\Theta) = b_q(\Theta)$$

The theorems below will relate the back-scattering data to the support of q . A glance at (1.6) makes it clear that it is impossible to produce an upper bound for the $\text{supp } q$. We will, however, compute a lower bound. We will associate (and compute numerically) with $b(\Theta)$, or $s(\Theta)$, its convex back-scattering support, a convex set which must be a subset of the convex hull of the support of any q which produces that back-scattering data. In the Born approximation we will also find a potential supported in any neighborhood of this set that reproduces the data. In this case, the convex back-scattering support is the unique smallest convex set that supports a potential that can produce this data.

We state all our theorems below, and will include only very brief descriptions of the necessary notation here, and defer both their detailed discussion and proofs to the following sections. In what follows, the symbol $\sigma_n(2kR)$ denotes the L^2 norm of the d -dimensional Bessel function of order n , and argument $2k|x|$, restricted to the ball of radius R . The number $N = N(n, d) \approx n^{d-2}$ denotes the dimension of the space of spherical harmonics of degree n . For a function $b \in L^2(S^{d-1})$, the functions $b_n^{(c)}(\Theta)$ represent the terms in the *condensed spherical harmonic expansion* (Fourier series expansion in 2 dimensions) of the function $e^{2i\Theta \cdot c} b(\Theta)$. Additionally, $B_c(R)$ denotes closed ball of radius R centered at the point $c \in \mathbb{R}^d$.

We now state our main results.

THEOREM 1.1 (Linear, Born-Back-Scattering). *Let $q \in L^2(\mathbb{R}^d)$ be compactly supported with Born-back-scattering kernel $b(\Theta)$, i.e.*

$$(1.7) \quad b(\Theta) := b_q(\Theta, -\Theta) = \frac{k^{d-2}}{2i} \widehat{q}(2k\Theta)$$

and let

$$e^{2ik\Theta \cdot c} b(\Theta) = \sum_{n=0}^{\infty} b_n^{(c)}(\Theta)$$

¹We will give a more precise mathematical description in the next section.

be its expansion in spherical harmonics centered at c . If the $\text{supp } q \subset B_c(R)$, then

$$(1.8) \quad \sum_{n=0}^{\infty} \frac{\|b_n^{(c)}\|_{L^2(S^{d-1})}^2}{\sigma_n^2(2kR)} < \infty$$

Conversely, if $b \in L^2(S^{d-1})$ satisfies (1.8), then there exists a $q \in L^2(\mathbb{R}^d)$ with $\text{supp } q \subset B_c(R)$ and Born-back-scattering kernel $b(\Theta)$.

Moreover, if $b \in L^2(S^{d-1})$ and \mathcal{B} denotes the collection of all balls, $B_c(R)$, for which (1.8) is satisfied, then for any $\epsilon > 0$, there exists $q \in C^\infty(\mathbb{R}^d)$ with ²

$$(1.9) \quad \text{supp } q \subset \mathcal{N}_\epsilon \left(\bigcap_{B_c(R) \in \mathcal{B}} B_c(R) \right)$$

and Born-back-scattering kernel equal to $b(\Theta)$.

THEOREM 1.2 (Nonlinear, Full Back-Scattering). *Let $q \in L^p(\mathbb{R}^d)$, where $p > \max(2, \frac{d}{2})$, be compactly supported with back-scattering kernel*

$$s(\Theta) := s_q(\Theta, -\Theta)$$

and let

$$e^{2ik\Theta \cdot c} s(\Theta) = \sum_{n=0}^{\infty} s_n^{(c)}(\Theta)$$

be its expansion in spherical harmonics centered at c . If the $\text{supp } q \subset B_c(R)$, then, for $n > \max(4R, 2R^2)$,

$$(1.10) \quad \|s_n^{(c)}\|_{L^2(S^{d-1})}^2 \leq C(q) N \sigma_n^2(2kR)$$

where $C(q)$ is given explicitly in (4.13).

If we observe that, for any $\epsilon > 0$, (1.10) implies (1.8) with R replaced by $R + \epsilon$, we obtain

COROLLARY 1.3. *If the $\text{supp } q \subset B_c(R)$, then there is a (complex-valued) $\tilde{q} \in C^\infty(\mathbb{R}^d)$ supported in an ϵ -neighborhood of $B_c(R)$ with Born-back-scattering kernel exactly equal to the full back-scattering kernel of q , i.e.*

$$b_{\tilde{q}}(\Theta) = s_q(\Theta)$$

As a consequence of these theorems, we define the convex scattering support to be

DEFINITION 1.4 (Convex Scattering Support).

$$\begin{aligned} \text{cS}_k \text{supp } b &= \bigcap_{B_c(R) \in \mathcal{B}} B_c(R) \\ \text{cS}_k \text{supp } s &= \bigcap_{B_c(R) \in \mathcal{S}} B_c(R) \end{aligned}$$

² $\mathcal{N}_\epsilon(\Omega)$ denotes an open ϵ -neighborhood of Ω , the set of points whose distance from Ω is less than ϵ .

where \mathcal{B} denotes the collection of balls such that b satisfies (1.8) and \mathcal{S} is the collection of balls such that s satisfies (1.10).

We record the main property of the convex scattering support below.

THEOREM 1.5. *In both the Born approximation and in the full back-scattering cases, the convex scattering support must be a subset of the convex hull of the support of any potential q with that back-scattering kernel.*

Proof. Merely note that any point that does not belong to the convex hull of the support of q can be separated from that set by a ball. The Hahn-Banach theorem tells us there is a separating hyper-plane, and because this convex set is bounded (q has compact support), a large enough ball will approximate the hyper-plane as close as necessary on any compact set and thus accomplish the separation.

□

In the Born approximation, the linear dependence on q allows a stronger statement.

THEOREM 1.6. *For any $b \in L^2(S^{d-1})$, the convex scattering support of the Born back-scattering kernel b is*

1. *The smallest convex set such that there is a q , supported in every neighborhood of that set, with Born back-scattering kernel b .*
2. *The largest convex set that is contained in the convex hull of the support of every q with Born back-scattering kernel equal to b .*

A simple consequence of theorem 1.6 is that the convex scattering support of a non-zero Born back-scattering kernel is non-empty. A consequence of corollary 1.3 is that this same conclusion holds for the full back-scattering kernel.

We introduced the convex scattering support of a far field of a source in [8] and [9]. We extended the notion to include fields scattered by a variation in wavespeed or an obstacle, in response to a single incident wave, and described one method to compute it. Different methods, that compute roughly the same set, have also appeared in [10],[13],[12],[4],[6], and [5].

Our main reason for extending the notion of convex scattering support to back-scattering is that the data is more realistically acquired, and therefore, the methods can be more readily adapted to be of practical use. To measure the far field of a single incident wave requires at least two sensors, one at a fixed position that radiates and another that will move around the scatterer to measure the field. Calibration requires accurate knowledge of the angle between the two devices, while back-scattering simply requires moving a single sensor.

It may appear that a condition like (1.10) is difficult to apply to noisy data. Exactly the opposite is true. The coefficients in a Fourier series or spherical harmonic expansion are easily computed. As we will point out in the final section, the function $\sigma_n(2kR)$, viewed as a function of n at a fixed value of $2kR$ is uniformly large for $n < 2kR$ and rapidly becomes uniformly small when $n > 2kR$. Thus, the norm of the terms in the spherical harmonic expansion for $e^{i2k\Theta \cdot c_S(\Theta)}$ undergo a rapid transition to, and become approximately, zero as n passes through the radius of the smallest ball that contains the convex scattering support. This transition is readily observable and remains so in the presence of appreciable noise.

2. The Herglotz, Far Field, and Scattering Operators. For any $\delta > \frac{1}{2}$, the unique $L^2_{-\delta}$ solution³ of the free (homogeneous) Helmholtz equation, parametrized by α , satisfies

$$(2.1) \quad (\Delta + k^2)v = 0$$

$$(2.2) \quad v \sim \frac{e^{ikr}}{r^{\frac{d-1}{2}}}\alpha(-\Theta) + \frac{e^{-ikr}}{r^{\frac{d-1}{2}}}\alpha(\Theta), \quad |x| = r \rightarrow \infty$$

and may be expressed in terms of the Herglotz operator

$$v(r\Phi) = (\mathcal{H}\alpha)(r\Phi) := k^{\frac{d-1}{2}} \int_{S^{d-1}} e^{ikr\Theta \cdot \Phi} \alpha(\Theta) d\Theta$$

The adjoint of the Herglotz operator, which maps $L^2_{\delta}(\mathbb{R}^d)$ into $L^2(S^{d-1})$, is therefore the Fourier transform (times a power of k), followed by restriction to the sphere of radius k , and may be written as

$$(2.3) \quad (\mathcal{H}^* f)(\Theta) = k^{\frac{d-1}{2}} \int_{\mathbb{R}^d} e^{-ikr\Theta \cdot \Phi} f(r\Phi) r^{d-1} dr d\Phi = k^{\frac{d-1}{2}} \widehat{f}(k\Theta)$$

Here we have simply written $d\Phi$ and $d\Theta$ rather than $dS(\Phi)$ and $dS(\Theta)$ to denote the surface measure on the unit sphere S^{d-1} .

We note that, for any right hand side $f \in L^2_{\delta}$, with $\delta > 1/2$, the source problem

$$(2.4) \quad (\Delta + k^2)u = f$$

has a unique *outgoing* solution. Such an *outgoing* solution has asymptotics similar to those in (2.2), however the second term vanishes. Specifically,

$$(2.5) \quad u \sim \frac{e^{ikr}}{r^{\frac{d-1}{2}}}\beta(\Theta) + \frac{e^{-ikr}}{r^{\frac{d-1}{2}}}\times 0, \quad |x| = r \rightarrow \infty$$

The function $\beta \in L^2(S^{d-1})$ is called the far field of the outgoing solution u . We will use the notation

$$u = Gf$$

to denote the solution operator which solves (2.4). Additionally, we define the far field operator \mathcal{F} as the map between the source f and the far field β , so that

$$\beta = \mathcal{F}f$$

We will make use of the fact that, except for a factor of $2ik$, the far field operator is the adjoint of the Herglotz operator, that is,

PROPOSITION 2.1.

$$\mathcal{F}f = \frac{1}{2ik} \mathcal{H}^* f = \frac{k^{\frac{d-3}{2}}}{2i} \widehat{f}(k\Theta)$$

³ $\|u\|_{L^2_{\delta}(\mathbb{R}^d)} = \|(1+|x|^2)^{\frac{\delta}{2}}u\|_{L^2(\mathbb{R}^d)}$. These spaces were first used in the context of the Helmholtz equation in [1] as a means for studying long-range potentials. The existence and uniqueness statements we quote here can be found in [8].

Proof. The second equality is a consequence of the first and (2.3). To establish the first, we apply Green's formula to u and v as previously defined in (2.4) and (2.1). I.e.,

$$\begin{aligned}
(\mathcal{H}\alpha, f) &= (v, f) \\
&= \int_{\mathbb{R}^d} \bar{v} f \\
&= \int_{\mathbb{R}^d} \bar{v}(\Delta + k^2)u - \overline{(\Delta + k^2)v}u \\
&= \lim_{R \rightarrow \infty} \int_{S_R^{d-1}} \left(\bar{v} \frac{\partial u}{\partial \nu} - \frac{\bar{\partial v}}{\partial \nu} u \right) d\Theta
\end{aligned}$$

which becomes, on inserting the asymptotics from (2.2) and (2.6)

$$\begin{aligned}
&= 2ik \int_{S^{d-1}} \bar{\alpha} \beta d\Theta \\
&= (\alpha, 2ik\mathcal{F}f)
\end{aligned}$$

□

In order to define the scattering operator, we return to (1.2)

$$(\Delta + k^2)u = qu$$

and seek u as an *outgoing* perturbation of the solution of the free Helmholtz equation with the incident field $\mathcal{H}\alpha$ so that

$$u = \mathcal{H}\alpha + u_{sc}$$

where u_{sc} is an outgoing solution. This means that u_{sc} is the unique outgoing solution of

$$(2.7) \quad (\Delta + k^2)u_{sc} = q\mathcal{H}\alpha + qu_{sc}$$

Such an outgoing field has the asymptotics

$$u_{sc} \sim \frac{e^{ikr}}{r^{\frac{d-1}{2}}} \beta_q(\Theta) + \frac{e^{-ikr}}{r^{\frac{d-1}{2}}} \times 0$$

This observation allows us to define the relative scattering operator

$$\mathcal{S}\alpha = \beta_q$$

The Born approximation replaces (2.7) with

$$(2.8) \quad (\Delta + k^2)u_{born} = q\mathcal{H}\alpha$$

The unique outgoing solution has the asymptotics

$$u_{born} \sim \frac{e^{ikr}}{r^{\frac{d-1}{2}}} \beta_{born}(\Theta) + \frac{e^{-ikr}}{r^{\frac{d-1}{2}}} \times 0$$

and so we define the (relative) Born scattering operator

$$\mathcal{B}\alpha = \beta_{born}$$

The Born scattering operator is the Fréchet derivative of the relative scattering operator with respect to q , evaluated at $q \equiv 0$. The factorizations below (similar to those in [7]) will enable us to derive useful properties of the scattering operator from analogous properties of the Herglotz operator.

PROPOSITION 2.2. *The full relative scattering operator admits the factorization*

$$(2.9) \quad \mathcal{S} = \frac{1}{2ik} \mathcal{H}^* q (I - Gq)^{-1} \mathcal{H}$$

$$(2.10) \quad = \frac{1}{2ik} \mathcal{H}^* (I - qG)^{-1} q \mathcal{H}$$

while the Born relative scattering operator may be decomposed as

$$(2.11) \quad \mathcal{B} = \frac{1}{2ik} \mathcal{H}^* q \mathcal{H}$$

The kernel of the Born relative scattering operator is

$$(2.12) \quad b(\Theta, \Phi) = \frac{k^{d-2}}{2i} \widehat{q}(k(\Theta - \Phi))$$

Proof. The proof below relies on the invertibility of $(I - qG)$, the proof of which we defer to lemma 4.1. We begin with (2.7) and apply G to both sides:

$$\begin{aligned} u_{sc} &= G(q\mathcal{H}\alpha + qu_{sc}) \\ (I - Gq)u_{sc} &= Gq\mathcal{H}\alpha \\ u_{sc} &= (I - Gq)^{-1} Gq\mathcal{H}\alpha \\ &= G(I - qG)^{-1} q\mathcal{H}\alpha \end{aligned}$$

so that the far field of u_{sc} is

$$\begin{aligned} \mathcal{S}\alpha &= \mathcal{F}(I - qG)^{-1} q\mathcal{H}\alpha \\ &= \frac{1}{2ik} \mathcal{H}^* (I - qG)^{-1} q\mathcal{H}\alpha \end{aligned}$$

establishing (2.9). The analogous calculation applied to (2.8) instead of (2.7) establishes (2.11). Once we know that $(I - qG)$ is invertible the identity

$$(I - qG)^{-1} q = q(I - Gq)^{-1}$$

follows from

$$q(I - Gq) = (I - qG)q$$

which transforms (2.10) into (2.9). Finally, writing the integral representation of (2.11) as

$$\begin{aligned} \mathcal{B}\alpha &= \frac{k^{d-2}}{2i} \int_{\mathbb{R}^d} e^{-irk\Psi \cdot \Phi} q(r\Psi) \left[\int_{S^{d-1}} e^{irk\Theta \cdot \Psi} \alpha(\Theta) d\Theta \right] r^{d-1} dr d\Psi \\ &= \frac{k^{d-2}}{2i} \int_{S^{d-1}} \left[\int_{\mathbb{R}^d} e^{-irk(\Phi - \Theta) \cdot \Psi} q(r\Psi) r^{d-1} dr d\Psi \right] \alpha(\Theta) d\Theta \end{aligned}$$

yields (2.12). \square

3. The Herglotz Operator and the Spherical Harmonics. In this and the next section, the notation will be slightly less cluttered if we restrict to the case $k = 1$. Because of the representations of the scattering operator in (2.9) and (2.10), the properties of the Herglotz operator will figure prominently into our analysis of the scattering operator. The singular value decomposition of the Herglotz operator in terms of the spherical harmonics and (spherical) Bessel functions will provide a basic tool for all our subsequent calculations. We begin with the expansion of an incident plane wave in spherical harmonics, which for $\Theta, \Phi \in S^{d-1}$ and $0 \leq r < \infty$, is

$$e^{ir\Theta \cdot \Phi} = \sum_{n=0}^{\infty} i^n j_n(r) p_n(\Theta \cdot \Phi)$$

The most useful way to define the functions p_n in our context is as the kernel of the orthogonal projection, \mathcal{P}_n , from $L^2(S^{d-1})$ onto the subspace of degree n spherical harmonics. I.e.

$$(\mathcal{P}_n \alpha)(\Theta) = \int_{S^{d-1}} p_n(\Theta \cdot \Phi) \alpha(\Phi) d\Phi$$

The functions $p_n(\Theta \cdot \Phi)$ play a dual role: they act as both kernels of projection operators and are themselves spherical harmonics. When we wish to emphasize their second role we will write

$$p_n^\Phi(\Theta) := p_n(\Theta \cdot \Phi)$$

Up to a constant, the function p_n^Φ is the unique spherical harmonic that is invariant under rotations about the Φ axis [11]. The constants involved here will be important to us, hence we compute

$$\begin{aligned} \mathcal{P}_n p_n^\Phi &= p_n^\Phi \\ \int_{S^{d-1}} p_n^\Psi(\Theta) p_n^\Phi(\Theta) d\Theta &= p_n^\Phi(\Psi) \end{aligned}$$

from which we learn that

$$\|p_n^\Psi\|_{L^2}^2 = p_n^\Psi(\Psi)$$

is independent of Ψ and

$$= \|p_n^\Psi\|_{L^\infty}$$

If we take the trace of the operator \mathcal{P}_n , we see that

$$\begin{aligned} \text{tr} \mathcal{P}_n &= \int_{S^{d-1}} p_n(\Theta \cdot \Theta) d\Theta \\ N &= p_n(\Theta \cdot \Theta) \omega \end{aligned}$$

where ω denotes the volume of the d -dimensional sphere and $N = N(n, d)$ the dimension of the space of spherical harmonics of degree n . Hence, we conclude that

$$\|p_n^\Phi\|_{L^2}^2 = \|p_n^\Phi\|_{L^\infty} = p_n^\Phi(\Phi) = \frac{N}{\omega}$$

In terms of the standard Legendre functions, P_n , we have the relation

$$p_n(\Theta \cdot \Phi) = \frac{N}{\omega} P_n(\Theta \cdot \Phi)$$

The Bessel functions $j_n(r)$ are most easily defined in terms of the Herglotz operator acting on the p_n 's. Recalling that $p_n^\Phi = p_n(\Theta \cdot \Phi)$ acts as both a spherical harmonic and the kernel of a projection, we see that

$$(3.1) \quad \begin{aligned} \mathcal{H}p_n^\Phi &= \int_{S^{d-1}} e^{ir\Theta \cdot \Psi} p_n(\Theta \cdot \Phi) d\Theta \\ &= \mathcal{P}_n e^{ir\Theta \cdot \Psi} \end{aligned}$$

so that $\mathcal{H}p_n^\Phi$, for each fixed r , must again be a spherical harmonic of degree n . We can check that the right hand side of (3.1) is invariant under rotations about the Φ -axis, and thus must be equal to a constant multiple of p_n^Φ itself. Specifically, this constant is i^n times the spherical Bessel function. I.e.

$$(3.2) \quad \mathcal{H}p_n^\Phi = i^n j_n(r) p_n^\Phi$$

Because the p_n 's act also as projection kernels, we see that any spherical harmonic of degree n may replace p_n^Φ in (3.2). The Herglotz operator is not compact. However, if we compose it with the restriction to the ball of radius R , the composition is compact. We denote the resulting operator by \mathcal{H}_R , and describe its singular value decomposition.

$$(3.3) \quad \begin{aligned} \mathcal{H}_R &= \sum_{n=0}^{\infty} \sigma_n(R) \frac{j_n^R(r)}{\|j_n^R\|} \mathcal{P}_n \\ &= \sum_{n=0}^{\infty} \sigma_n(R) \mathcal{Q}_n \end{aligned}$$

We have used the notation j_n^R to denote the Bessel function multiplied by the characteristic function of $B_0(R)$, the ball of radius R centered at 0, and defined the singular values

$$\sigma_n^2(R) := \|j_n\|_{L^2(B_0(R))}^2$$

Each projection operator

$$\mathcal{Q}_n := \frac{j_n^R(r)}{\|j_n^R\|} \mathcal{P}_n$$

is an isometry from the N -dimensional space of spherical harmonics of degree n in $L^2(S^{d-1})$ to an N dimensional subspace of $L^2(B_0(R))$. In short, we find that the \mathcal{Q}_n 's simply project onto the spherical harmonics of degree n and then multiply the result by $\frac{j_n^R(r)}{\|j_n^R\|}$.

Since the singular values all have multiplicity greater than one, this looks a little different than the more familiar version of the singular value decomposition. A compact linear operator K admits the representation

$$(3.4) \quad \begin{aligned} K &= \sum_{n=0}^{\infty} \lambda_n \Psi_n \otimes \Phi_n \\ &= \sum_{n=0}^{\infty} \lambda_n \tilde{\mathcal{Q}}_n \end{aligned}$$

In this case, Ψ_n and Φ_n are orthonormal basis vectors so that the tensor products $\tilde{Q}_n = \Psi_n \otimes \Phi_n$ are isometries between one-dimensional subspaces.

The corresponding singular value decomposition for the operator \mathcal{H}_R^* is

$$(3.5) \quad \mathcal{H}_R^* = \sum_{n=0}^{\infty} \sigma_n(R) \mathcal{Q}_n^*$$

and the ranges of the \mathcal{Q}_n^* are exactly the subspaces of spherical harmonics of degree n . Note that, as no $\sigma_n(R)$ is zero, \mathcal{H}_R^* has dense range in $L^2(S^{d-1})$.

Now, we recall

THEOREM 3.1 (Picard's Theorem). *If $K : X \rightarrow Y$ is a compact linear operator with dense range in Y and has a singular value decomposition of the form given in (3.4), then*

$$\alpha = Kf$$

if and only if

$$\sum_{n=0}^{\infty} \frac{\|\mathcal{Q}_n \alpha\|^2}{\lambda_n^2} < \infty$$

and $\alpha \in N(K^*)^\perp$. The proof of theorem 1.1 is now in hand.

Proof. [Proof of theorem 1.1] The second equality in (1.7) follows from (2.12) on setting $\Phi = -\Theta$. Now, scaling the Fourier transform gives

$$b(\Theta) = \frac{1}{2i} \widehat{q}(2\Theta) = 2^{-d} \mathcal{H}^* q(x/2)$$

The Picard theorem applied to \mathcal{H}_R^* tells us that, in the case $c = 0$, if the $\text{supp } q \subset B_c(R)$, then b satisfies (1.8). It also tells us the converse, that if b satisfies (1.8), there exists a $q \in L^2(\mathbb{R}^d)$ with $\text{supp } q \subset B_c(R)$ and Born-back-scattering kernel $b(\Theta)$.

The Fourier shift theorem tells us that the Fourier transform – and therefore \mathcal{H}^* and \mathcal{H}_R^* – intertwines translation by c and multiplication by $e^{ik\Theta \cdot c}$, i.e.

$$e^{ik\Theta \cdot c} \mathcal{H}^* q = \mathcal{H}^* T_c q := \mathcal{H}^* q(x - c)$$

which establishes the corresponding conclusions for arbitrary c .

So far we have shown that every ball for which (1.8) is satisfied supports a q with Born-back-scattering kernel b . We now wish to demonstrate that any open neighborhood of their intersection supports such a q as well. As a consequence of lemma 3.2, given below, we find that if each of two convex sets support potentials q with corresponding Born-back-scattering kernel b , then so must any neighborhood of their intersection.

LEMMA 3.2. *Suppose the $\text{supp } q_1 \subset \Omega_1$, the $\text{supp } q_2 \subset \Omega_2$ and that $\mathbb{R}^d \setminus (\Omega_1 \cup \Omega_2)$ is connected and contains a neighborhood of ∞ . If*

$$(3.6) \quad \mathcal{H}^* q_1 = \mathcal{H}^* q_2 = b$$

then, for any $\varepsilon > 0$, there exists an $q_3 \in C^\infty(\mathbb{R}^d)$ with

$$\text{supp } q_3 \subset \mathcal{N}_\varepsilon(\Omega_1 \cap \Omega_2)$$

and

$$\mathcal{H}^* q_3 = b$$

Proof. A consequence of (3.6) is that the outgoing solutions of

$$(\Delta + (2k)^2) u_i = q_i, \quad i = 1, 2$$

$u_1 = Gq_1$ and $u_2 = Gq_2$ have the same far field. According to Rellich's lemma and the unique continuation principle [2], u_1 and u_2 also agree on the $\mathbb{R}^d \setminus (\Omega_1 \cup \Omega_2)$. Let $\phi \in C^\infty(\mathbb{R}^d)$ satisfy

$$\phi = \begin{cases} 1, & x \in \mathbb{R}^n \setminus \mathcal{N}_\varepsilon(\Omega_1 \cap \Omega_2) \\ 0, & x \in \mathcal{N}_{\frac{\varepsilon}{2}}(\Omega_1 \cap \Omega_2) \end{cases}$$

then,

$$v = \begin{cases} \phi u_1, & x \in \mathbb{R}^d \setminus \Omega_1 \\ \phi u_2, & x \in \mathbb{R}^d \setminus \Omega_2 \\ 0, & x \in \Omega_1 \cap \Omega_2 \end{cases}$$

is a well-defined C^∞ function and $v = u_1 = u_2$ outside a compact set so that

$$q_3 = (\Delta + (2k)^2)v$$

must also have $\mathcal{H}^* q_3 = b$. \square

Because the intersection of convex sets is convex, and the complement of the union of two convex sets must be connected, the lemma can be applied repeatedly to produce a $q \in C^\infty$ satisfying the (apparently weaker) analog of (1.9) with \mathcal{B} replaced by any finite collection of balls, $B_c(R)$, for which (1.8) holds. The following compactness argument shows that (1.9) follows from this analog. Let R_0 be large enough that $\mathcal{N}_\varepsilon(\bigcap_{B_c(R) \in \mathcal{B}} B_c(R)) \subset B_0(R_0)$, then $B_0(R_0) \setminus \mathcal{N}_\varepsilon(\bigcap_{B_c(R) \in \mathcal{B}} B_c(R))$ is a compact set covered by the relatively open subsets $B_0(R_0) \setminus B_c(R)$, so a finite sub-collection, $\mathcal{B}_\mathcal{M}$, of these open subsets suffices to cover that compact set, i.e.

$$(3.7) \quad B_0(R_0) \setminus \mathcal{N}_\varepsilon\left(\bigcap_{B_c(R) \in \mathcal{B}} B_c(R)\right) \subset \bigcup_{B_c(R) \in \mathcal{B}_\mathcal{M}} \left(B_0(R_0) \setminus B_c(R)\right)$$

Taking complements of this inclusion yields

$$\mathcal{N}_\varepsilon\left(\bigcap_{B_c(R) \in \mathcal{B}} B_c(R)\right) \supset \bigcap_{B_c(R) \in \mathcal{B}_\mathcal{M}} B_c(R)$$

from which we conclude that (1.9) follows from its apparently weaker analog. This finishes the proof of theorem 1.1. \square

4. Estimating the Full Back-Scattering Kernel. This section is composed of three main propositions, and a few supporting lemmas, which combine to prove theorem 1.2. We begin with the following lemma concerning the invertibility of the operator $I - Gq$.

LEMMA 4.1. *Let $q \in L^\infty(\mathbb{R}^d)$ and be compactly supported. Then $q(I - Gq)^{-1}$ is a bounded operator from $L^2(\mathbb{R}^d)$ to itself. Moreover, let $q \in L^p(\mathbb{R}^d)$, with $p > \max(2, \frac{d}{2})$, be compactly supported. Then,*

$$q(I - Gq)^{-1} = q + Gq(I - Gq)^{-1}$$

and $Gq(I - Gq)^{-1}$ and $(I - Gq)^{-1}$ are bounded operators from $L^2(\mathbb{R}^d)$ to itself.

Proof. The lemma is a special consequence of lemma 12, and corollaries 13, 14, and 15 of [9]. Roughly speaking, multiplication by q loses $\frac{d}{p}$ L^2 -derivatives while G gains two. This implies that Gq is compact and that $I - Gq$ is Fredholm. If zero were an eigenvalue of $I - Gq$, then the corresponding eigenfunction would be a nonzero outgoing solution to (1.2). An application of Green's formula to this solution and its complex conjugate shows that this outgoing solution would have zero far field. Rellich's lemma and unique continuation imply that any outgoing solution with zero far field is identically zero. Thus zero is not an eigenvalue and $I - Gq$ is invertible. \square

PROPOSITION 4.2. *If $q \in L^\infty$, the $\text{supp } q \subset B_c(R)$, then scattering operator may be factored as*

$$(4.1) \quad \mathcal{S} = e^{-i\Theta \cdot c} \mathcal{H}_R^* B \mathcal{H}_R e^{i\Theta \cdot c}$$

where B is a bounded operator from $L^2(\mathbb{R}^d)$ to itself.

Proof.

Because \mathcal{H} intertwines translation by c and multiplication by $e^{ik\Theta \cdot c}$, i.e.

$$\mathcal{H} e^{-i\Theta \cdot c} = T_c \mathcal{H}$$

it is enough to treat the case $c = 0$. We begin with (2.10),

$$\mathcal{S} = \mathcal{H}^* (I - qG)^{-1} q \mathcal{H}$$

then, insert a characteristic function of the ball

$$(4.2) \quad = \mathcal{H}^* (I - qG)^{-1} q \chi_R \mathcal{H}$$

then, shift to (2.9)

$$= \mathcal{H}^* q (I - Gq)^{-1} \chi_R \mathcal{H}$$

and again insert another characteristic function

$$(4.3) \quad = \mathcal{H}^* \chi_R q (I - Gq)^{-1} \chi_R \mathcal{H}$$

which we recognize as

$$(4.4) \quad = \mathcal{H}_R^* q (I - Gq)^{-1} \mathcal{H}_R$$

Finally, we observe that the operator in the middle is bounded according to lemma 4.1. \square

REMARK 4.3. *The only property of the scattering operator that we will use in the sequel is (4.1). The conclusions of theorem 1.2 apply to any operator which admits such a factorization.*

REMARK 4.4. *So as not to unnecessarily complicate the subsequent discussion, we will continue working with $q \in L^\infty$ in the rest of this section. Theorem 1.2, however,*

remains true for compactly supported $q \in L^p(\mathbb{R}^d)$ with $p > \max(2, \frac{d}{2})$. In this case, the scattering operator is the sum of two operators,

$$(4.5) \quad \begin{aligned} \mathcal{S} &= \mathcal{H}_R^* q (I - Gq)^{-1} \mathcal{H}_R \\ &= \mathcal{H}_R^* q \mathcal{H}_R + \mathcal{H}_R^* Gq (I - Gq)^{-1} \mathcal{H}_R \end{aligned}$$

The first is the Born scattering operator and the second satisfies (4.1) with a $B = Gq(I - Gq)^{-1}$ which is bounded from $L^2(\mathbb{R}^d)$ to itself.

The factorization (4.1) combines with the singular values of the Herglotz operator to give some natural estimates for the terms in what we might call a *block decomposition* of the scattering operator.

PROPOSITION 4.5. *Let \mathcal{S} , mapping $L^2(S^{d-1})$ to itself, admit the factorization (4.1), then \mathcal{S}_{nm} , defined as*

$$(4.6) \quad \mathcal{S}_{nm} = \mathcal{P}_n \mathcal{S} \mathcal{P}_m$$

has an L^∞ kernel $s_{nm}(\Theta, \Phi)$, and satisfies

$$(4.7) \quad \begin{aligned} \|\mathcal{S}_{nm}\| &\leq \sigma_n(R) \sigma_m(R) \|B\| \\ |s_{nm}(\Theta, \Phi)| &\leq \sqrt{N} \sigma_n(R) \sqrt{M} \sigma_m(R) \|B\| \end{aligned}$$

Proof. We insert the factorization (4.1) into (4.6)

$$\begin{aligned} \mathcal{S}_{nm} &= \mathcal{P}_n \mathcal{H}_R^* B \mathcal{H}_R \mathcal{P}_m \\ &= (\mathcal{H}_R \mathcal{P}_n)^* B \mathcal{H}_R \mathcal{P}_m \end{aligned}$$

and use our singular value decompositions, (3.3) and (3.5)

$$(4.8) \quad = \sigma_n \sigma_m \mathcal{Q}_n^* B \mathcal{Q}_m$$

so that

$$\|\mathcal{S}_{nm}\| \leq \sigma_n \sigma_m \|B\|$$

Recalling again that the p_n^Θ 's are kernels of the \mathcal{P}_n 's, we see that the kernel of \mathcal{S}_{nm} , is given by

$$\begin{aligned} s_{nm}(\Theta, \Phi) &= (p_n^\Theta, \mathcal{S} p_m^\Phi)_{L^2(S^{d-1})} \\ &= (p_n^\Theta, \mathcal{S}_{nm} p_m^\Phi)_{L^2(S^{d-1})} \\ |s_{nm}(\Theta, \Phi)| &\leq \|p_n^\Theta\| \|\mathcal{S}_{nm}\| \|p_m^\Phi\| \\ &\leq \sqrt{N} \sigma_n(R) \sigma_m(R) \|B\| \sqrt{M} \end{aligned}$$

□

The main conclusion of theorem 1.2 is the estimate (1.10) of the left hand side of the identity (4.9) below. We will apply (4.7) to show that the series on the right hand side is summable, and then to prove (1.10).

$$(4.9) \quad \mathcal{P}_l \mathcal{S}(\Theta, -\Theta) = \sum_{n,m} \mathcal{P}_l \mathcal{S}_{nm}(\Theta, -\Theta)$$

The next proposition tells us that many of the terms in the series are zero.

PROPOSITION 4.6.

$$\mathcal{P}_l(s_{nm}(\Theta, -\Theta)) \equiv 0$$

unless the sum of any two indices is greater than or equal to the third.

Proof.

$$\begin{aligned} s_{nm}(\Theta, -\Theta) &= (p_n^{-\Theta}, \mathcal{S}p_m^\Theta)_{L^2(S^{d-1})} \\ &= \left(\int_{S^{d-1}} p_n(\Theta \cdot \Psi_1) p_n^{\Psi_1} d\Psi_1, \mathcal{S} \int_{S^{d-1}} p_m(\Theta \cdot \Psi_2) p_m^{\Psi_2} d\Psi_2 \right) \\ &= \int_{S^{d-1}} \int_{S^{d-1}} p_n(\Theta \cdot \Psi_1) p_m(\Theta \cdot \Psi_2) (p_n^{\Psi_1}, \mathcal{S}p_m^{\Psi_2}) d\Psi_1 d\Psi_2 \\ \mathcal{P}_l s_{nm}(\tau) &= \int_{S^{d-1}} \int_{S^{d-1}} \left[\int_{S^{d-1}} p_l(\Theta \cdot \tau) p_n(\Theta \cdot \Psi_1) p_m(\Theta \cdot \Psi_2) d\Theta \right] (p_n^{\Psi_1}, \mathcal{S}p_m^{\Psi_2}) d\Psi_1 d\Psi_2 \end{aligned}$$

The quantities in the square brackets are closely related to the Clebsch-Gordon coefficients [14]. To see that they must be zero, fix Ψ_1 and Ψ_2 , and call the quantity in the square brackets $c_{nml}(\tau)$. Since $p_l^\tau(\Theta) = p_l(\Theta \cdot \tau)$ is the kernel of the projection operator \mathcal{P}_l onto degree l spherical harmonics, we see that $c_{nml}(\tau)$ are the degree l spherical harmonics in the condensed spherical harmonic expansion of the product of the two spherical harmonics, $p_n^{\Psi_1}$ and $p_m^{\Psi_2}$. I.e.

$$p_n^{\Psi_1}(\Theta) p_m^{\Psi_2}(\Theta) = \sum_{l=0}^{\infty} c_{nml}(\Theta)$$

Recalling that every spherical harmonic extends to a homogeneous polynomial of the same degree, we see that the left hand side extends to the unit ball as a homogeneous polynomial of degree $n + m$ if we replace Θ by $r\Theta$. Since the left hand side goes to zero as r^{n+m} as $r \rightarrow 0$, so must the right hand side. This is only possible if the c_{nml} , which extend as homogeneous degree l polynomials, are zero for all $l < n + m$. Finally, note that all conclusions remain valid if we permute the indices n , m , and l . \square

Proof. [Proof of Theorem 1.2]

We start by applying propositions 4.2 and 4.5 to conclude that

$$(4.10) \quad |s_{nm}(\Theta, \Phi)| \leq \|q(I - Gq)^{-1}\| \sqrt{N} \sigma_n(R) \sqrt{M} \sigma_m(R)$$

We set $\Phi = -\Theta$ and let $s_{nm}(\Theta) = s_{nm}(\Theta, -\Theta)$.

Now, (4.10) tells us that the terms $|s_{nm}(\Theta)|$ are summable. Hence, we may write

$$s(\Theta) = \sum_{n,m=0}^{\infty} s_{nm}(\Theta)$$

and therefore

$$\mathcal{P}_l s(\Theta) = \sum_{n,m=0}^{\infty} \mathcal{P}_l s_{nm}(\Theta)$$

which is the same as

$$= \sum_{n+m \geq l} \mathcal{P}_l s_{nm}(\Theta)$$

according to proposition 4.6. Hence

$$(4.11) \quad \begin{aligned} \|\mathcal{P}_l s\|_{L^2} &\leq \sum_{n+m \geq l} \|\mathcal{P}_l s_{nm}(\Theta)\|_{L^2} \\ &\leq \sum_{n+m \geq l} \|s_{nm}(\Theta)\|_{L^2} \end{aligned}$$

Recalling that ω is the area of S^{d-1}

$$(4.12) \quad \begin{aligned} &\leq \sqrt{\omega} \sum_{n+m \geq l} \|s_{nm}(\Theta)\|_{L^\infty} \\ &\leq \sqrt{\omega} \|q(I - Gq)^{-1}\| \sum_{n+m \geq l} \sqrt{N} \sigma_n(R) \sqrt{M} \sigma_m(R) \end{aligned}$$

Finally, proposition 4.7, which we state and prove below, estimates the sum on the right hand side in terms of $\sigma_l(2R)$.

$$(4.13) \quad \leq \|q(I - Gq)^{-1}\| \frac{\omega \sqrt{2} R^{\frac{d}{2}}}{(1 - \frac{2R}{l})(1 - \frac{R^2}{l + \frac{d}{2}})^2} \sqrt{L} \sigma_l(2R)$$

This completes the proof for $q \in L^\infty$. For $q \in L^p(\mathbb{R}^d)$ with $p > \max(2, \frac{d}{2})$, we return to (4.5) and notice that theorem 1.2 holds for each of the two terms. It holds for the first because it is a Born back-scattering kernel and for the second because the operator in the middle is bounded. It is not hard to see that the conclusion will persist for the sum. \square

The next proposition provides an estimate of the right hand side of equation (4.13) and thus yields the last ingredient necessary to establish theorem 1.2.

PROPOSITION 4.7.

$$(4.14) \quad \sum_{n+m \geq l} \sqrt{N} \sigma_n(R) \sqrt{M} \sigma_m(R) \leq \frac{\sqrt{2\omega} R^{\frac{d}{2}}}{(1 - \frac{2R}{l})(1 - \frac{R^2}{l + \frac{d}{2}})^2} \sqrt{L} \sigma_l(2R)$$

Proof. The proof requires several small lemmas. The first allows us to estimate the $\sigma_n(r)$'s from above and below by ratios of Γ -functions and powers of r .

LEMMA 4.8.

$$(4.15) \quad \frac{\Gamma(\frac{d}{2})(\frac{r}{2})^n}{\Gamma(n + \frac{d}{2})} \left(1 - \frac{(\frac{r}{2})^2}{n + \frac{d}{2}}\right) \leq j_n(r) \leq \frac{\Gamma(\frac{d}{2})(\frac{r}{2})^n}{\Gamma(n + \frac{d}{2})}$$

$$(4.16) \quad \frac{\sqrt{\omega} 2^{\frac{d-1}{2}} \Gamma(\frac{d}{2})(\frac{r}{2})^{n+\frac{d}{2}}}{\Gamma(n + \frac{d+1}{2})} \left(1 - \frac{(\frac{r}{2})^2}{n + \frac{d}{2}}\right) \leq \sigma_n(r) \leq \frac{\sqrt{\omega} 2^{\frac{d}{2}} \Gamma(\frac{d}{2})(\frac{r}{2})^{n+\frac{d}{2}}}{\Gamma(n + \frac{d+1}{2})}$$

Proof. The first inequality, (4.15), is just the statement that the spherical Bessel function lies between the first and the partial sum of the first two terms of its alternating power series expansion. The second is obtained from the first by squaring, integrating over the ball of radius r , and making use of (4.18) below. \square

The dimensions N of the spaces of spherical harmonics of degree n also appear on the left hand side of (4.14). We will estimate them from above and below in terms of Γ -functions as well.

LEMMA 4.9.

$$N(n, d) = \begin{cases} 1 & n = 0 \\ d & n = 1 \\ \frac{(2n+d-2)(n+d-3)!}{n!(d-2)!} & \text{otherwise} \end{cases}$$

$$(4.17) \quad \frac{\Gamma(n+d-1)}{\Gamma(n+1)\Gamma((d-1))} \leq N \leq 2 \frac{\Gamma(n+d-1)}{\Gamma(n+1)\Gamma(d-1)}$$

Proof. The first formula follows from the observation that N satisfies the difference equation

$$N(n, d) = N(n, d-1) + N(n-1, d)$$

and the fact that (4.17) holds in the special cases $n = 0$ and $d = 2$. See [11] for a different proof. The inequality (4.17) follows from this formula and

$$n+d-2 \leq 2n+d-2 \leq 2(n+d-2)$$

□ The ratio $\frac{s!}{(s-1)!} = \frac{\Gamma(s+1)}{\Gamma(s)} = s$. We need to estimate the analogous ratio when one of the arguments is a half integer. For this we state

LEMMA 4.10.

$$(4.18) \quad \left(s - \frac{1}{2}\right)^{\frac{1}{2}} \leq \frac{\Gamma(s + \frac{1}{2})}{\Gamma(s)} \leq s^{\frac{1}{2}}$$

Proof. Because the gamma function is log-convex [3],

$$\begin{aligned} \Gamma\left(s + \frac{1}{2}\right) &\leq \Gamma(s)^{\frac{1}{2}} \Gamma(s+1)^{\frac{1}{2}} \\ \frac{\Gamma\left(s + \frac{1}{2}\right)}{\Gamma(s)} &\leq \frac{\Gamma(s+1)^{\frac{1}{2}}}{\Gamma(s)^{\frac{1}{2}}} = s^{\frac{1}{2}} \end{aligned}$$

Analogously,

$$\begin{aligned} \Gamma(s) &\leq \Gamma\left(s - \frac{1}{2}\right)^{\frac{1}{2}} \Gamma\left(s + \frac{1}{2}\right)^{\frac{1}{2}} \\ \frac{\Gamma(s)}{\Gamma\left(s + \frac{1}{2}\right)} &\leq \frac{\Gamma\left(s - \frac{1}{2}\right)^{\frac{1}{2}}}{\Gamma\left(s + \frac{1}{2}\right)^{\frac{1}{2}}} = \frac{1}{\left(s - \frac{1}{2}\right)^{\frac{1}{2}}} \end{aligned}$$

□ We use lemma 4.10 to establish a replacement for the binomial theorem involving Γ -functions of half integers rather than just factorials.

LEMMA 4.11.

$$\sum_{n+m=l} \frac{1}{\Gamma\left(n + \frac{d+1}{2}\right)} \frac{1}{\Gamma\left(m + \frac{d+1}{2}\right)} \leq \frac{2^{l+d-1}}{\Gamma(l+d)}$$

Proof. If d is odd, the inequality is an equality which follows from the binomial expansion of $(1+1)^{l+d-1}$. If d is even, we use (4.18)

$$\begin{aligned}
\sum_{n+m=l} \frac{1}{\Gamma(n + \frac{d+1}{2})} \frac{1}{\Gamma(m + \frac{d+1}{2})} &\leq \sum_{n+m=l} \frac{(n + \frac{d}{2})^{\frac{1}{2}}}{\Gamma(n + \frac{d}{2} + 1)} \frac{(m + \frac{d}{2})^{\frac{1}{2}}}{\Gamma(m + \frac{d}{2} + 1)} \\
&\leq (l + \frac{d}{2}) \sum_{n+m=l} \frac{1}{\Gamma(n + \frac{d}{2} + 1)} \frac{1}{\Gamma(m + \frac{d}{2} + 1)} \\
&= (l + \frac{d}{2}) \frac{2^{l+d}}{\Gamma(l+d+1)} \\
&\leq \frac{2^{l+d}}{\Gamma(l+d)}
\end{aligned}$$

□

The sum in (4.14) is in fact a double summation over the indices n and m . Hence, we first estimate each single sum in lemma 4.12 below, and then sum those estimates in lemma 4.13 to estimate the double summation.

LEMMA 4.12.

$$\sum_{n+m=l} \sqrt{N} \sigma_n(R) \sqrt{M} \sigma_m(R) \leq \frac{\sqrt{2\omega} R^{\frac{d}{2}}}{(1 - \frac{R^2}{l+\frac{d}{2}})} \sqrt{L} \sigma_l(2R)$$

Proof.

$$\sum_{n+m=l} \sqrt{N} \sigma_n(R) \sqrt{M} \sigma_m(R) \leq L \sum_{n+m=l} \sigma_n(R) \sigma_m(R) \tag{4.19}$$

We apply (4.15) from lemma 4.8

$$\leq \omega 2^{d-1} \Gamma^2\left(\frac{d}{2}\right) \left(\frac{R}{2}\right)^{l+d} L \sum_{n+m=l} \frac{1}{\Gamma(n + \frac{d+1}{2})} \frac{1}{\Gamma(m + \frac{d+1}{2})}$$

then lemma 4.11

$$\leq \omega 2^{d-1} \Gamma^2\left(\frac{d}{2}\right) \left(\frac{R}{2}\right)^{l+d} L \frac{2^{l+d}}{\Gamma(l+d)}$$

followed by the left inequality in (4.16) of lemma 4.8

$$(4.20) \quad \leq \frac{\sqrt{\omega} \sqrt{L} \sigma_l(2R)}{(1 - \frac{R^2}{l+\frac{d}{2}})} \left(2^{\frac{d-1}{2}} \left(\frac{R}{2}\right)^{\frac{d}{2}}\right) \left(\Gamma\left(\frac{d}{2}\right) \sqrt{L} \frac{\Gamma(l + \frac{d+1}{2})}{\Gamma(l+d)}\right)$$

and finally (4.17) to see that the third factor in (4.20) is less than 2

$$(4.21) \quad \leq \frac{\sqrt{\omega} \sqrt{L} \sigma_l(2R)}{(1 - \frac{R^2}{l+\frac{d}{2}})} \left(2^{\frac{d+1}{2}} \left(\frac{R}{2}\right)^{\frac{d}{2}}\right)$$

□ Finally, we complete these estimates with

LEMMA 4.13.

$$(4.22) \quad \sum_{l=l_0}^{\infty} \sqrt{L} \sigma_l \leq \frac{\sqrt{L_0} \sigma_{l_0}}{(1 - \frac{R}{l_0})(1 - \frac{R^2}{4l_0+2d})}$$

Proof.

$$\sum_{l=l_0}^{\infty} \sqrt{L} \sigma_l \leq \sqrt{L_0} \sigma_{l_0} \left(1 + \sum_{l=l_0+1}^{\infty} \sqrt{\frac{L}{L_0}} \frac{\sigma_l}{\sigma_{l_0}} \right)$$

According to lemma 4.9

$$\leq \sqrt{L_0} \sigma_{l_0} \left(1 + \sum_{k=1}^{\infty} \sqrt{\frac{\Gamma(l_0 + k + d - 1) \Gamma(l_0 + 1)}{\Gamma(l_0 + d - 1) \Gamma(l_0 + k + 1)}} \frac{\sigma_l}{\sigma_{l_0}} \right)$$

Estimating the square root gives,

$$(4.23) \quad \leq \sqrt{L_0} \sigma_{l_0} \left(1 + \sum_{k=1}^{\infty} \left(1 + \frac{d-2}{l_0+1} \right)^{\frac{k}{2}} \frac{\sigma_l}{\sigma_{l_0}} \right)$$

(4.24)

Next, we apply both upper and lower bounds in (4.16) of lemma 4.8,

$$(4.25) \quad \leq \sqrt{L_0} \sigma_{l_0} \left(1 + \sum_{k=1}^{\infty} \left(1 + \frac{d-2}{l_0+1} \right)^{\frac{k}{2}} \left(\frac{R}{2} \right)^k \frac{\Gamma(l_0 + \frac{d+1}{2})}{\Gamma(l_0 + k + \frac{d+1}{2})} \frac{1}{1 - \frac{R^2}{4l_0+2d}} \right)$$

(4.26)

and finally estimate the ratio of Gamma functions, and compare to a geometric series,

$$(4.27) \quad \begin{aligned} &\leq \sqrt{L_0} \sigma_{l_0} \left(1 + \sum_{k=1}^{\infty} \left(1 + \frac{d-2}{l_0+1} \right)^{\frac{k}{2}} \frac{\left(\frac{R}{2} \right)^k}{\left(l_0 + \frac{d+1}{2} \right)^k} \frac{1}{1 - \frac{R^2}{4l_0+2d}} \right) \\ &\leq \frac{\sqrt{L_0} \sigma_{l_0}}{1 - \frac{R^2}{4l_0+2d}} \left(1 + \sum_{k=1}^{\infty} \left(\frac{\left(1 + \frac{d-2}{l_0+1} \right)^{\frac{1}{2}} r}{l_0 + \frac{d+1}{2}} \right)^k \right) \\ &\leq \frac{\sqrt{L_0} \sigma_{l_0}}{1 - \frac{R^2}{4l_0+2d}} \sum_{k=0}^{\infty} \left(\frac{r}{l_0} \frac{\sqrt{1 + \frac{d-2}{l_0+1}}}{1 + \frac{d+1}{2l_0}} \right)^k \\ &\leq \frac{\sqrt{L_0} \sigma_{l_0}}{1 - \frac{R^2}{4l_0+2d}} \sum_{k=0}^{\infty} \left(\frac{r}{l_0} \right)^k \end{aligned}$$

Hence, (4.22) follows on summing the geometric series. \square

We need only observe that combination of lemmas 4.12 and 4.13 implies (4.14) to finish the proof of proposition 4.7. \square

5. Numerical Applications. In this section, we illustrate a method for finding the convex back-scattering support with a simple example in two dimensions. Here, our scatterer is rectangle R_q ,

$$R_q = \{(x, y) \in \mathbb{R}^2 : -1 \leq x \leq 1, -1/2 \leq y \leq 1/2\}$$

having horizontal sides at $x = \pm 1$ and vertical ones at $y = \pm 0.5$. We computed the full (not the Born) back-scattering kernel numerically, using the Helmholtz equation

$$(\Delta + k^2 n^2(x))u = 0$$

with the wavenumber $k = 5$ and index of refraction given by the formula

$$n^2 = \begin{cases} 2 & x \in R_q \\ 1 & x \notin R_q \end{cases}$$

5.1. The Forward Solution. In this section we explain how we computed the back-scattering kernel that we will use as data to numerically determine the convex back-scattering support for our example to follow.

For each incident wave, we employ a two-step process. First, we solved a discretized version of the Lippmann-Schwinger integral equation (LSIE) for the total field u on (a region slightly larger than) the support of the scatterer, using a Nyström, or collocation, method. Next, we use the product qu as a source and numerically integrate it against the two dimensional version of the far field operator \mathcal{F} , computing only the value of the scattered field in the direction opposite that of the incident wave.

More specifically, we solved the LSIE numerically by discretizing the operator $I - Gq$, and the incident wave u^i , over a large, but finite, number of nodes on a prescribed rectangular region $D = D_x \times D_y$ containing the scatterer q and then solved the ensuing large system of simultaneous equations (of the form $Au = u^i$) for the unknown u on our grid of evaluation nodes. This process was then repeated over a collection of incident directions on the unit circle.

In two dimensions, we use a collection of equally spaced points $(x_l, y_p) \in D$, ($l = 1, 2, \dots, M, p = 1, 2, \dots, N$), and then express the LSIE as

$$u(\hat{x}_l, \hat{y}_p) + \int_{D_x} \int_{D_y} K(\hat{x}_l - x, \hat{y}_p - y)u(x, y)dydx = u^i(\hat{x}_l, \hat{y}_p)$$

where the kernel K is

$$K(\hat{x}_l - x, \hat{y}_p - y) = \frac{i}{4}H_0^{(1)}\left(k\sqrt{(\hat{x}_l - x)^2 + (\hat{y}_p - y)^2}\right)q(x, y)$$

and $H_0^{(1)}$ is the usual Hankel function of the first kind. We discretize the points of integration similarly, defining the additional points (x_l, y_p) , at the same points of evaluation of the LSIE. Using the Trapezoid-Rule on this same set of nodes allows us to write the fully discrete version of the LSIE as

$$u_{\hat{l}, \hat{p}} + \frac{\Delta x \Delta y}{4} \sum_{\substack{p=1 \\ p \neq \hat{p}}}^{N-1} \sum_{\substack{l=1 \\ l \neq \hat{l}}}^{M-1} (K_{\hat{l}, l; \hat{p}, p} u_{l, p} + K_{\hat{l}, l+1; \hat{p}, p} u_{l+1, p} + K_{\hat{l}, l; \hat{p}, p+1} u_{l, p+1} \\ + K_{\hat{l}, l+1; \hat{p}, p+1} u_{l+1, p+1}) + w_{\hat{l}, \hat{p}} S_{\hat{l}, \hat{p}} u_{\hat{l}, \hat{p}} = u_{\hat{l}, \hat{p}}^i$$

The notation given above has been abbreviated so that the subscripts indicate the points of evaluation. Namely, $u_{\hat{l}, \hat{p}} = u(\hat{x}_l, \hat{y}_p)$, $u_{l, p} := u(x_l, y_p)$, and $K_{\hat{l}, l; \hat{p}, p} = K(\hat{x}_l - x_l, \hat{y}_p - y_p)$. Since the kernel of the integral operator is singular along the diagonal, these terms must be treated separately in the discretization scheme. The term $w_{\hat{l}, \hat{p}} S_{\hat{l}, \hat{p}} u_{\hat{l}, \hat{p}}$ above corresponds to the appropriate Trapezoid-Rule weighted average of

the diagonal terms in the discretization. Specifically,

$$S_{\hat{l}, \hat{p}} := \begin{cases} \frac{k^2}{4} \delta^2 q_{\hat{l}, \hat{p}} (1 - 2 \log \delta - 4C_k) & \text{if } (\hat{x}_l, \hat{y}_p) \in D \\ \frac{k^2}{8} \delta^2 q_{\hat{l}, \hat{p}} (1 - 2 \log \delta - 4C_k) & \text{if } (\hat{x}_l, \hat{y}_p) \in \partial D. \end{cases}$$

where

$$C_k = \frac{1}{2} \left(\log \frac{k}{2} - \gamma \right) - \frac{i\pi}{4}$$

and γ is the Euler-Mascheroni constant.

In more detail, what we have done is to assume that product qu is nearly constant over some small ball of radius δ and integrated the logarithmic singularity of the kernel on this set to define the appropriate matrix entry in the numerical integration along the diagonal. Provided we take a fine mesh of integration points, this presents a viable way to treat this weakly singular behavior. We use an equi-spaced grid in both x and y and chose δ to be $\Delta x/2$.

Lastly, we obtained the back-scattered field by simply computing the discrete sum of the form

$$s_q(\theta) = e^{i\frac{5\pi}{4}} \sqrt{\frac{1}{8k\pi}} \sum_{l=1}^{M-1} (A_l(\theta) + A_{l+1}(\theta)) \frac{\Delta x}{2}$$

where we define the iterated areas $A_l(\theta)$ and $A_{l+1}(\theta)$ as

$$A_l(\theta) = \sum_{p=1}^{N-1} (f(x_l, y_p, \theta) + f(x_l, y_{p+1}, \theta)) \frac{\Delta y}{2}$$

$$A_{l+1}(\theta) = \sum_{p=1}^{N-1} (f(x_{l+1}, y_p, \theta) + f(x_{l+1}, y_{p+1}, \theta)) \frac{\Delta y}{2}$$

and where we used the computed values of the total field u on the grid to compute

$$f(x_l, y_p, \theta) = e^{-ik(x_l \cos \theta + y_p \sin \theta)} q(x_l, y_p) u(x_l, y_p)$$

Again, we ran the above numerical scheme for a rectangular scatterer, i.e. $q = k^2 \chi_{R_q}$ with χ_{R_q} the characteristic function of the rectangle

$$R_q = \{(x, y) \in \mathbb{R}^2 : -1 \leq x \leq 1, -1/2 \leq y \leq 1/2\}$$

and computed the back-scattering kernel at 100 equi-spaced points on the unit circle. We used a wavenumber of $k = 5$ and distributed 40 nodes along each of the x and y axes within the bounding region

$$D = \{(x, y) \in \mathbb{R}^2 : -1 \leq x \leq 1, -1 \leq y \leq 1\}$$

Just over 1.5 wavelengths fall within D , so that 40 Trapezoidal-rule integration nodes (roughly 25 nodes per wavelength) should yield an accurate simulated solution.

5.2. Numerical Computation of the Convex Back-Scattering Support.

In this section, we illustrate how we use the back-scattering data to find the rectangle⁴. The general outline of our method for locating the rectangle from the back-scattering kernel will be the following:

1. Choose a center, $c \in \mathbb{R}^2$ (we take $c = 0$ the first time through) and expand the back-scattering kernel in a Fourier series centered at this point.
2. Find the *support*, i.e. the value of n where these coefficients *rapidly transition to zero*, in order to calculate the radius of the smallest ball centered at c that contains the (convex back-scattering support of the) rectangle. We will explain this in detail below.
3. Choose other centers and repeat the above process to produce other balls.
4. The scatterer, e.g. the rectangle, must be contained in the common intersection of all these balls.

The second step warrants further explanation. We begin by expanding the back-scattering kernel, i.e. the measured back-scattered signal, in a Fourier series centered at c . On the circle, it is more convenient to work with the azimuthal angle $\theta \in [0, 2\pi]$, which is related to the unit vector Θ through $\Theta = (\cos \theta, \sin \theta)$. The Fourier series expansion, centered at c , is

$$e^{ic \cdot \Theta} s(\Theta) = \sum_{n=-\infty}^{\infty} t_n e^{in\theta}$$

Numerically, we compute a finite sequence $\{t_n\}$ as the discrete Fourier transform of the sequence $\{e^{ic \cdot \Theta_n} s(\Theta_n)\}$, where $\{\Theta_n\}$ are equi-spaced points on the unit circle. In theorem 1.2 we expanded in condensed spherical harmonics. In two dimensions, the condensed spherical harmonics of degree n are the linear combinations of $e^{in\theta}$ and $e^{-in\theta}$, i.e., $s_0^{(c)}(\Theta) = t_0$ and

$$(5.1) \quad s_n^{(c)}(\Theta) = t_n e^{in\theta} + t_{-n} e^{-in\theta}, \quad n \geq 1$$

so that $\|s_0^{(c)}\|_{L^2(S^1)} = |t_0|$ and

$$(5.2) \quad \|s_n^{(c)}\|_{L^2(S^1)} = (|t_{-n}|^2 + |t_n|^2)^{\frac{1}{2}}, \quad n \geq 1$$

Now, if the scatterer, i.e. our rectangle, is contained in the ball of radius R , then, the s_n 's satisfy the estimate (1.10), which simplifies slightly in two dimensions because $N(n, 2) = 2$. Specifically,

$$\|s_n^{(c)}\|_{L^2(S^1)} \leq C(q)N\sigma_n(2kR) \leq 2C(q)\sigma_n(2kR)$$

Theorem 1.2 only tells us that, if the rectangle is contained in the ball of radius R centered at c , then the s_n 's (a shorthand notation for the $\|s_n^{(c)}\|_{L^2}$) are bounded by a constant times the $\sigma_n(2kR)$'s. We shall operate as if we knew the converse were true as well⁵. The wavenumber k is fixed ($k = 5$ in the example below), so we want to examine the s_n 's and find the smallest value of R for which such a bound holds. Our test principle for finding R from the Fourier coefficients will be the following:

⁴In general, we can only expect to find the convex back-scattering support of the scatterer, which may be smaller than the convex hull of the scatterer. In the Born approximation, it follows from theorem 14 of [8] that the convex back-scattering support of a rectangle is exactly the rectangle. We have not proved this for the full back-scattering data, but the numerical computations below suggest that this is the case.

⁵For the Born approximation, the converse is part of theorem 1.1.

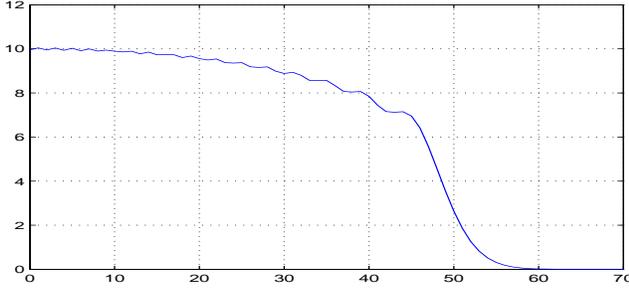


FIG. 1. $\sigma_n(50)$ plotted as a function of n . Notice that $\sigma_n(50)$ is large (> 6) for $n < 45$ and small (< 0.5) for $n > 55$. If we knew only that this was a plot of $\sigma_n(R)$ for some R , we could have deduced an approximation for R by finding the value of n where the function rapidly transitioned to zero.

TEST PRINCIPLE 5.1. *The s_n 's are effectively supported in the interval $(0, N)$ if and only if the the convex back-scattering support is contained in the ball of radius $R = \lfloor \frac{N}{2k} \rfloor$.*

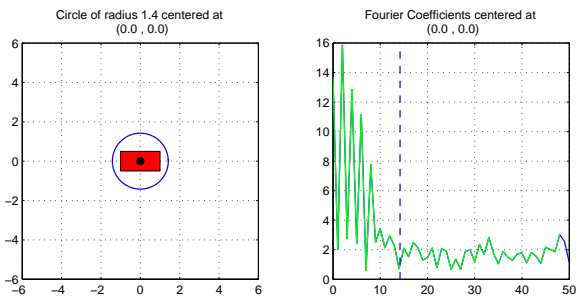
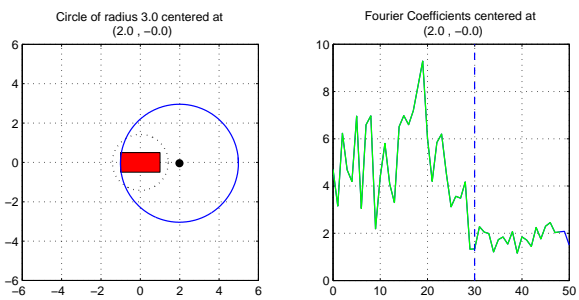
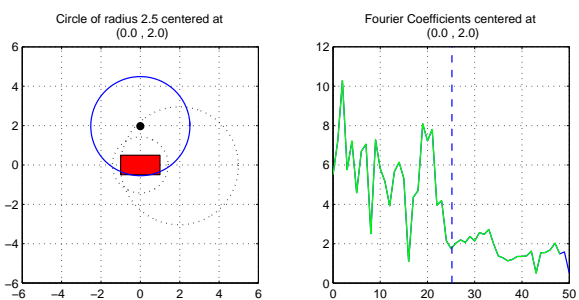
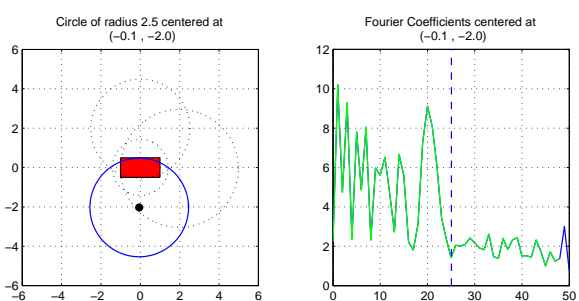
We expect the s_n 's to be effectively supported in the interval $(0, N)$ because the $\sigma_n(2kR)$'s have exactly this property. As a function of n , $\sigma_n(2kR)$ is positive and bounded away from zero for $n < |2kR|$ and effectively zero for $n > |2kR|$, with a transition region of width proportional to $(2kR)^{1/3}$. We see evidence of this behavior in the graph of $\sigma_n(50)$ in figure 1 and in the asymptotic formulas:

$$(5.3) \quad \sigma_n(2kR) \sim \begin{cases} \sqrt{2} \left((2kR)^2 - n^2 \right)^{\frac{1}{4}} & n < |2kR| \\ \left(\frac{ekR}{n} \right)^{n+1} \sim 0 & n > |2kR| \end{cases}$$

Equation (5.3) follows from classical asymptotics of Bessel functions when at least one of either n or kR is large. We don't yet know a proof when neither is large, but rely on numerical computations in this case. It can be shown that the two sequences, $\sigma_{2n}(2kR)$ and $\sigma_{2n+1}(2kR)$ are monotone decreasing as $n > 0$ increases.

The sequences of graphs on the following two pages illustrate the transitions we witness in the σ_n 's are also observed in the back-scattering data as well.

Plots	Comments
	<ul style="list-style-type: none"> • We plot the modulus of the Fourier coefficients of the back-scattering kernel on the right and locate the transition to zero at $n = 13$, indicating that value of n by the dashed vertical line. • We draw the deduced circle of radius $\frac{n}{2k} = \frac{13}{2 \times 5}$ on the left, including the rectangle for comparison.
	<ul style="list-style-type: none"> • We choose a new center, indicated by the black dot in the plot on the left. • We compute the modulus of the translated Fourier coefficients, plot them on the right, and locate the transition to zero at $n = 32$. • We draw the deduced circle of radius $\frac{n}{2k} = \frac{32}{2 \times 5}$ in the plot on the left. The dashed line represents the previous circle.
	<ul style="list-style-type: none"> • We choose another new center, indicated by the black dot. We again plot the modulus of the translated coefficients, locate the transition to zero at $n = 28$, and draw the new circle. • The dashed lines represent the previous circles. Recall that the back-scattering support must lie in their intersection.
	<p>We chose the sequence of centers so that we could approximate the rectangle with just a few circles, and thus illustrate the method with only a few plots. Of course, we based this choice on a priori knowledge. We don't discuss strategies for efficiently choosing the centers. One alternative is to simply test all centers on some grid of interest.</p>

Plots	Comments
 <p>Circle of radius 1.4 centered at (0.0, 0.0)</p> <p>Fourier Coefficients centered at (0.0, 0.0)</p>	<p>This sequence of plots uses the same data as the previous sequence, but we have added white noise to both the the amplitude and phase of the data. We chose the noise level to be 15% (i.e. variance equal to 0.15 times maximum amplitude (16) of the original data for the amplitudes and $0.15 \times 2\pi$ for the phases).</p>
 <p>Circle of radius 3.0 centered at (2.0, -0.0)</p> <p>Fourier Coefficients centered at (2.0, -0.0)</p>	<ul style="list-style-type: none"> • We locate the <i>transition to the noise level</i> rather than the transition to zero. • If we didn't know that the noise level was 2.4 (0.15×16), we could readily estimate it from any of the four plots.
 <p>Circle of radius 2.5 centered at (0.0, 2.0)</p> <p>Fourier Coefficients centered at (0.0, 2.0)</p>	<ul style="list-style-type: none"> • Our estimates of the radii in the noisy case are consistently smaller than in the noiseless case.
 <p>Circle of radius 2.5 centered at (-0.1, -2.0)</p> <p>Fourier Coefficients centered at (-0.1, -2.0)</p>	<ul style="list-style-type: none"> • We believe that the last two plots exhibit a single, more rapid transition than the first two because the distance from any point in the rectangle to the center of the circle does not vary much compared with the variation in the first two plots.

As illustrated in the previous collection of plots, our test principle is based on a transition which occurs at a finite value of n , while the theorems 1.1 and 1.2 depend only on large n asymptotics. The strict conditions of these theorems may never be verified experimentally, while the test principle, or any condition that does not include a limit as $n \rightarrow \infty$, can not be mathematically correct. One can always construct a potential q , supported in the ball of radius R , having any finite number of Fourier coefficients of $\hat{q}(k\Theta)$ equal to an arbitrary set of numbers. This set of numbers can be – somewhat artificially – chosen to be identically zero or to mimic the transition we seek, and thus foil our test principle. Nonetheless, such an example would always be exposed by increasing the wavenumber. Theoretically, we can use a wave of any fixed wavelength to probe any medium – even one which varies very rapidly as a function of position on the scale of that wavelength – to discover its convex back-scattering support. Practically speaking, however, we can not expect to effectively probe a medium whose features vary rapidly on the scale of a wavelength. Some dichotomy between theory and practice is inevitable. One goal for future work will be a more accurate description of those media that we can confidently test with this data and this method.

We should also mention that there are certainly other reasonable, and perhaps better, methods for deducing R than our proposed test principle 5.1. For instance, one might attempt to sum a regularized version of the series given in (1.8) over various values of R and seek the value of R where the sum becomes bigger than some prescribed threshold. We use the principle 5.1 above since the very steep transition remained easily visible in the presence of noise. This is not a property that the partial summations we tried shared. For our proposed test scheme, we did not need to choose a regularization parameter; however, we did need to decide where the transition to zero, or to the observable noise level, occurred. We found the transition by eye.

REFERENCES

- [1] S. Agmon. Spectral properties of schrödinger operators and scattering theory. *Annali della Scuola Normale Superiore di Pisa*, 2(2):151–218, 1975.
- [2] D. Colton and R. Kress. *Inverse Acoustic and Electromagnetic Scattering Theory*. Springer-Verlag, 1998.
- [3] L. Hörmander. *Notions of convexity*, volume 127 of *Progress in Mathematics*. Birkhäuser Boston Inc., Boston, MA, 1994.
- [4] M. Ikehata. On reconstruction in the inverse conductivity problem with one measurement. *Inverse Problems*, 16(3):785–793, 2000.
- [5] M. Ikehata. The probe method and its applications. In *Inverse problems and related topics (Kobe, 1998)*, volume 419 of *Chapman & Hall/CRC Res. Notes Math.*, pages 57–68. Chapman & Hall/CRC, Boca Raton, FL, 2000.
- [6] M. Ikehata. A regularized extraction formula in the enclosure method. *Inverse Problems*, 18(2):435–440, 2002.
- [7] A. Kirsch. Factorization of the far-field operator for the inhomogeneous medium case and an application in inverse scattering theory. *Inverse Problems*, 15:413–429, 1999.
- [8] S. Kusiak and J. Sylvester. The scattering support. *Comm. Pure Appl. Math.*, 56(11):1525–1548, 2003.
- [9] S. Kusiak and J. Sylvester. The scattering support in a non-uniform background. *SIAM Journal of Mathematical Analysis*, 36(4):1142–1158, 2005.
- [10] D. R. Luke and R. Potthast. The no response test—a sampling method for inverse scattering problems. *SIAM J. Appl. Math.*, 63(4):1292–1312 (electronic), 2003.
- [11] C. Müller. *Analysis of Spherical Symmetries in Euclidean Spaces*. Springer-Verlag, 1998.
- [12] R. Potthast. A set-handling approach for the no-response test and related methods. *Math. Comput. Simulation*, 66(4-5):281–295, 2004.
- [13] R. Potthast, J. Sylvester, and S. Kusiak. A ‘range test’ for determining scatterers with unknown physical properties. *Inverse Problems*, 19(3):533–547, 2003.

- [14] E. P. Wigner. *Group theory: And its application to the quantum mechanics of atomic spectra*. Expanded and improved ed. Translated from the German by J. J. Griffin. Pure and Applied Physics. Vol. 5. Academic Press, New York, 1959.